optica

Monolithic 56 Gb/s silicon photonic pulse-amplitude modulation transmitter: supplementary material

Chi Xiong*, Douglas M. Gill, Jonathan E. Proesel, Jason S. Orcutt, Wilfried Haensch, William M.J. Green

IBM T.J. Watson Research Center, 1101 Kitchawan Road, Yorktown Heights, New York 10598, USA
Corresponding author: cxiong@us.ibm.com

Published 21 September 2016

This document provides supplementary information to "Monolithic 56 Gb/s silicon photonic pulse-amplitude modulation transmitter," http://dx.doi.org/10.1364/optica.3.001060. Details of the optimization of the traveling-wave modulators are provided.

http://dx.doi.org/10.1364/optica.3.001060.s001

1. OPTIMIZATION OF THE PAM-4 WAVEFORM

Since both sections of the PAM-4 modulator operate in traveling-wave mode, the RF performance of the modulators are susceptible to RF reflections due to impedance mismatch. To investigate the effects of different termination resistance on the performance of the modulator, the termination of the traveling-wave electrode in our designs is made of a network of parallel resistors whose wiring can be cut in the top metal level using focused-ion beam to yield 20, 30, 40, or 50 Ω impedance (Fig. S1(a)).

The frequency response of the electro-optic (EO) modulation is analytically calculated based on a model adapted from [1], which accounts for all major contributions to the frequency response: RF loss, velocity mismatching and impedance mismatching. Experimentally measured RF attenuation ($\alpha_m = 45\sqrt{f}(\text{dB}/\sqrt{Hz}\cdot \text{cm})$), optical group index ($n_{g,o} = 3.6$), RF group index ($n_{g,RF} = 3.5$) and characteristic impedance of the transmission line ($Z_o = 30\Omega$) are used in the model. Fig.S1(b) shows the simulated frequency response of the long section of the PAM-4 modulator as a function of the termination resistor value (Z_t).

Fig.S1(b) shows that the impact of the termination resistance on the modulator EO response is most significant at frequencies below 10 GHz. The magnitude of the EO response at frequencies higher than 10 GHz is approximately the same for all termination values. When $Z_t < Z_o$, the EO response below 10 GHz is suppressed, effectively increasing the modulation bandwidth. This behavior has been reported previously [2]. While a lower Z_t will increase the modulation bandwidth, the time-domain waveform is optimized when termination impedance is perfectively matched to the characteristic impedance of the transmission line, $Z_t = Z_o$.

Fig.S2 shows three NRZ eye diagrams experimentally measured on the long segment of the PAM-4 MZM with termination resistance of 20, 30 and 40 Ω respectively. The eye diagrams are taken at a low bit rate of 10 Gbaud to better contrast the ringing features within the longer bit time period. Although not as clearly visualized, the effects are similar at 25 Gbaud. When the termination is at 20 Ω (upper eye), which is low, undershoot ringing is visible on the bit transition edge. When the termination is at 40 Ω (lower eye), which is high, overshoot ringing is observed. The eye is only optimized when the termination resistor is matched to the characteristic impedance of the transmission line (30 Ω, middle eye).

The degradation due to impedance mismatch has a larger effect in a PAM-4 waveform than it does in an NRZ waveform because the overshoot and undershoot ringing have excursions into the neighboring eyes in a PAM-4 waveform and reduce eye openings. To illustrate the effect, we compare the experimental eye diagrams of two PAM-4 transmitter, one with a lower (20 Ω) termination, and another with a well-matched (30 Ω) termination (Fig. S3). In Fig.S3 (a), for 20 Ω termination, both the vertical and horizontal eye openings are reduced because of overshoot excursions into neighboring eyes. For the case of a 30 Ω termination (Fig. S3(b)), which is matched to the transmission line, the openings of the three eyes are significantly improved.

REFERENCES

1. K. Kubota, J. Noda, and O. Mikami, "Traveling wave optical modulator using a directional coupler $LiNbO_3$ waveguide," Quantum Electronics, IEEE Journal of **16**, 754–760 (1980).
2. H. Yu and W. Bogaerts, "An equivalent circuit model of the traveling wave electrode for carrier-depletion-based silicon optical modulators," Journal of Lightwave Technology **30**, 1602–1609 (2012).

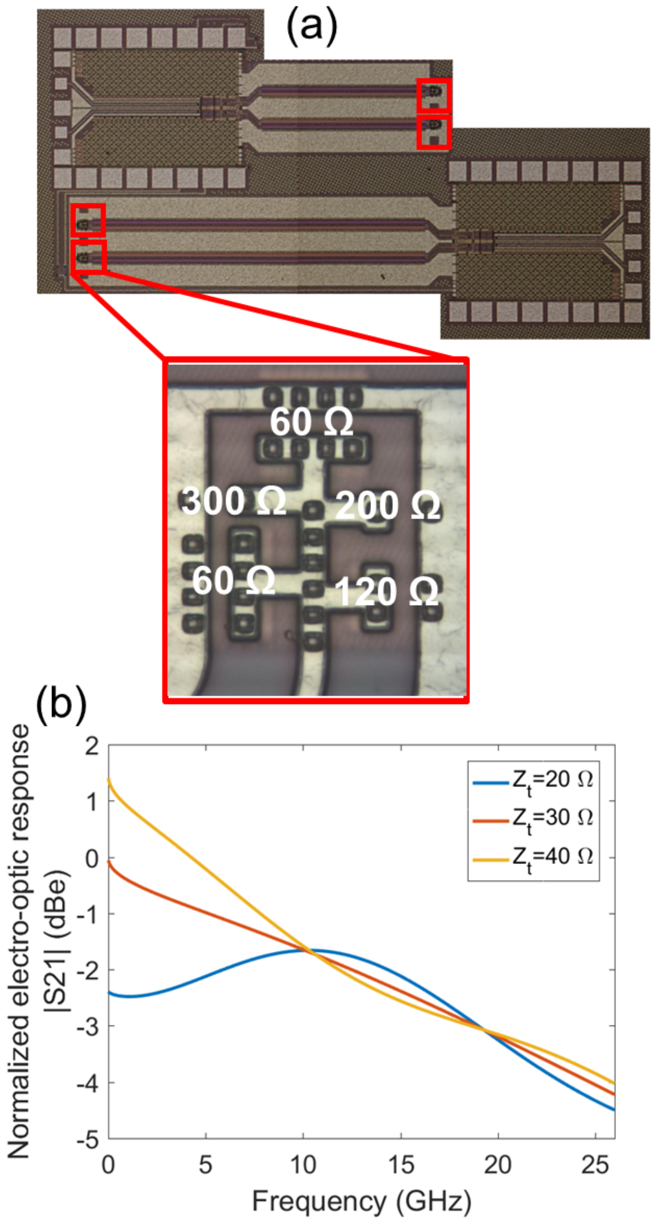

Fig. S1. (a) Micrograph of the PAM-4 transmitter. The four red squares highlight the location of the termination resistor network, which is magnified in the inset. The termination of both MZM segments consist of a network of five parallel resistors (60, 60, 120, 200, and 300 Ω), which can be cut using focused-ion beam to yield 20, 30, 40 or 50 Ω. (b) Theoretical electro-optic |S21| response for the long MZM segment for termination values of 20, 30 and 40 Ω respectively. The measured characteristic impedance of the transmission line (Z_o) is 30 Ω.

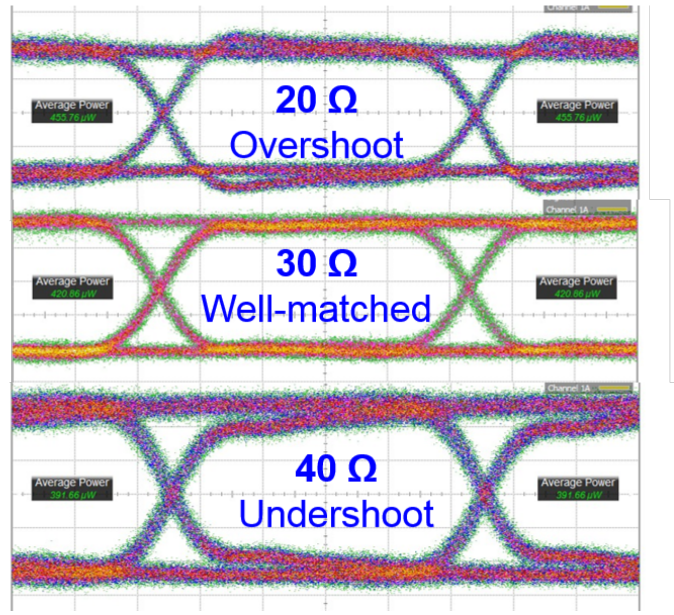

Fig. S2. The measured 10 Gbaud eye diagrams from the long segment of the PAM-4 modulator for 20 (low), 30 (well-matched) and 40 Ω (high) termination, which cause overshoot, well-matched and undershoot features during bit transitions.

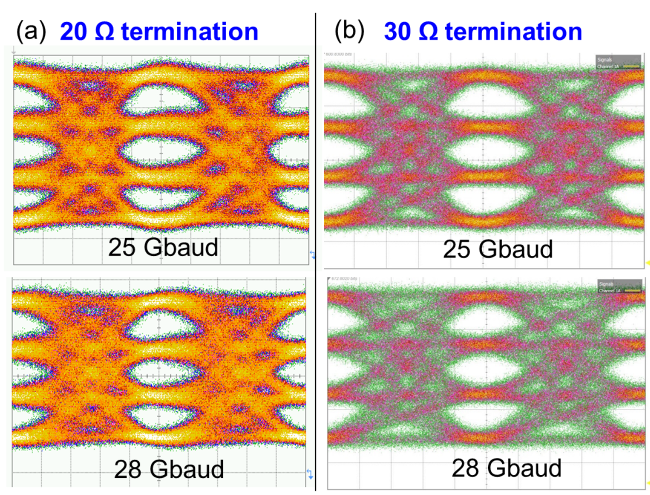

Fig. S3. (a) PAM-4 waveforms at 25 Gbaud (top) and 28 Gbaud (bottom) respectively for termination resistance value of 20 Ω; (b) PAM-4 waveforms at 25 Gbaud (top) and 28 Gbaud (bottom) respectively for termination resistance value of 30 Ω. All the eye diagrams are taken with $2^{31} - 1$ bit PRBS.